

---

## Axonal processes and neural plasticity. III. Competition for dendrites

T. Elliott, C. I. Howarth and N. R. Shadbolt

*Phil. Trans. R. Soc. Lond. B* 1997 **352**, 1975-1983  
doi: 10.1098/rstb.1997.0183

---

### Email alerting service

Receive free email alerts when new articles cite this article - sign up in the box at the top right-hand corner of the article or click [here](#)

---

To subscribe to *Phil. Trans. R. Soc. Lond. B* go to: <http://rstb.royalsocietypublishing.org/subscriptions>

---

# Axonal processes and neural plasticity. III

## Competition for dendrites

T. ELLIOTT\*, C. I. HOWARTH AND N. R. SHADBOLT

*Department of Psychology, University of Nottingham, Nottingham NG7 2RD, UK*  
([te@proteus.psyc.nott.ac.uk](mailto:te@proteus.psyc.nott.ac.uk))

### CONTENTS

	PAGE
1. Introduction	1975
2. Materials and methods	1976
3. Results	1978
4. Discussion	1980
Appendix 1. Statistical forces	1981
References	1982

### SUMMARY

In previous work we have developed a computational framework for topographic map formation and plasticity based on axonal process sprouting and retraction, in which sprouting and retraction are governed by competition for neurotrophic support. Here we show that such an approach can account for certain aspects of the dendritic morphology of cortical maps. In particular, we model the development of ocular dominance columns in the primary visual cortex and show that cortical cells near to column boundaries prefer to elaborate dendritic fields which avoid crossing the boundaries. This emerges as different functional inputs are spatially separated. We predict that afferent segregation occurs before or simultaneously with, but not after, the emergence of dendritic bias. We predict that animals reared with complete but asynchronous stimulation of the optic nerves do not develop a dendritic bias. We suggest that the emergence of a dendritic bias might provide a partial account for the critical period for a response to monocular deprivation. In particular, we predict that animals reared with asynchronous optic nerve stimulation might exhibit an extended critical period. Our results also indicate that the number of synapses supported by cortical cells depends on the intra-ocular image correlations used in our simulations. This suggests that inter-ocular image correlations, and thus strabismic rearing of kittens, may also affect the innervation density.

### 1. INTRODUCTION

Ocular dominance columns (Hubel & Wiesel 1962) form during a critical period in development (Hubel & Wiesel 1970) during which activity-dependent competition between the two eyes for cortical space leads to an anatomical segregation of geniculocortical afferents (Levay *et al.* 1978, 1980). Accumulating evidence implicates retrograde neurotrophic factors, particularly the neurotrophin gene family of neurotrophic factors, as possible mediators of activity-dependent competitive anatomical rearrangement in the visual system. For example, intraventricular infusion of nerve growth factor tempers the effects of monocular deprivation in the kitten visual cortex (Carmignoto *et al.* 1993), and cortical application of the neurotrophin NT-4/5, but no other neurotrophin, prevents the atrophy of lateral geniculate nucleus (LGN) cells in the ferret in response to monocular deprivation (Riddle *et al.* 1995). In addition, infusion of either brain-derived neurotrophic factor (BDNF)

or NT-4/5 in the kitten visual cortex prevents the anatomical segregation of geniculocortical afferents (Cabelli *et al.* 1995). Furthermore, the expression of BDNF mRNA in the rat visual cortex is activity dependent, since either dark rearing or monocular deprivation cause a rapid decrease in its level (Castren *et al.* 1992; Bozzi *et al.* 1995; Schoups *et al.* 1995). Finally, the complexity of retinotectal afferent arbors in *Xenopus* has been shown to be a function of the supply of BDNF (Cohen-Cory & Fraser 1995). These results are consistent with a model of activity-dependent anatomical competition in which afferents compete for a limited supply of neurotrophic factors, and in which, when the supply is not limited, competition between afferents is tempered or eliminated (see, for example, Purves 1988). The N-methyl-D-aspartate glutamate receptor also plays a role in activity-dependent competition (Kleinschmidt *et al.* 1987; Bear & Coleman 1990; Bear *et al.* 1990), perhaps by regulating the levels of target-derived neurotrophins (Zafra *et al.* 1991; Gwag & Springer 1993).  
The anatomical rearrangement of afferents during

\* Author for correspondence.

the development of ocular dominance columns affects the morphology of target cell dendritic fields in both the monkey (Katz *et al.* 1989) and the cat (Kossel *et al.* 1995) and also in the three-eyed frog (Katz & Constantine-Paton 1988). At the boundaries separating different columns, there is a distinct bias for the dendrites of a cell whose soma is in one column to remain in that column, leading to asymmetric dendritic fields. This bias is enhanced in strabismic cats (Kossel *et al.* 1995), suggesting that the dendritic re-modelling is activity dependent. While the mechanisms of dendritic re-modelling are largely unknown, preliminary evidence suggests that neurotrophic factors may be involved (Snider 1988; McAllister *et al.* 1995, 1996).

Most computational models of the formation of ocular dominance columns and related structures consider only an anatomically fixed network of variable strength connections. Many of these employ synaptic normalization, in which the total synaptic strength supported by a neuron is taken to be (roughly) fixed, in order to enforce competition between afferents (Von der Malsburg 1973). Experimentally, however, there is very little evidence to support the idea of synaptic normalization. Other fixed anatomy models modify the Hebb rule so that afferents which fire a post-synaptic cell above (below) its recent, average firing rate automatically undergo an increase (decrease) in synaptic strength and thus avoid imposing synaptic normalization (Bienenstock *et al.* 1982; Clothiaux *et al.* 1991). Some sprouting and retraction models have also been presented (Von der Malsburg 1979; Fraser & Perkel 1989; Montague *et al.* 1991). While these avoid the 'selectionist' prejudice (Purves 1994) of fixed anatomy models, they do not consider the role of neurotrophic factors in activity-dependent competition.

In a series of papers (Elliott *et al.* 1996*a-c*) we have developed a sprouting and retraction framework for cortical map formation and plasticity based on competition for neurotrophic factors. To date we have modelled the development of ocular dominance columns, the plasticity of adult somatosensory maps, and various pharmacological manipulations of the developing visual system, such as the infusion of muscimol, a  $\gamma$ -aminobutyric acid receptor agonist (Hata & Stryker 1994) and BDNF (Cabelli *et al.* 1995) into the primary visual cortex. Our approach is grounded in statistical mechanics and has similarities to the work of Hopfield (1982). However, while Hopfield uses statistical mechanics to find new states of activation in an anatomically fixed network, we use statistical mechanics to determine new patterns of connectivity in a network whose activity may also be varying. Also, Tanaka (1991) has presented an elegant model of ocular dominance column formation based on statistical mechanics, but it employs synaptic stabilization (Changeux & Danchin 1976) and so does not permit the principled growth of new connections. Here we wish to elaborate our approach further by showing that a sprouting and retraction model based on competition for neurotrophic support can naturally account for the dendritic bias observed in

the monkey and cat primary visual cortex (Katz *et al.* 1989; Kossel *et al.* 1995).

The plan for the remainder of the paper is as follows. We present our framework for sprouting and retraction. Next we present simulation results. Finally we discuss our results.

## 2. MATERIALS AND METHODS

In this section we describe our approach and the use of statistical mechanics for simulating what we shall take to be the stochastically fluctuating pattern of connectivity between the LGN and the primary visual cortex. By modelling sprouting and retraction in this way, we are able to set to one side the mechanisms underlying sprouting and retraction, about which there is great experimental uncertainty.

The LGN is taken to be composed of two regular, periodic  $r \times r$  arrays of  $r^2$  cells each, one array controlled by the left eye (the 'left LGN sheet') and the other by the right eye (the 'right LGN sheet'). Each LGN cell supports an axon from which emerge axonal processes forming synaptic connections with the cortex. All synaptic efficacies are taken to be fixed and equal; this is justified since we wish to model anatomical, not physiological, segregation. The LGN cells project topographically to the cortex, with each cell arborizing over a preferred patch of cortex only. The cortex is taken to be a regular periodic  $c \times c$  array of  $c^2$  cells, with each cell supporting a regular  $d \times d$  array of  $d^2$  dendrites. Thus, the cortex is a regular periodic  $cd \times cd$  array of  $c^2 d^2$  dendrites. While axons are allowed to sprout and retract, the positions of dendrites are fixed relative to the cortical array. The arbor region of an axon is a regular  $a \times a$  array of cortical cells. Initially each axon supports  $a^2 d^2$  processes uniformly distributed throughout its arbor region, one process attached to each of the  $a^2 d^2$  dendrites in the region. Each axon must always support at least  $a^2 d^2$  processes; there are no other limits on connectivity. The letters  $i$  and  $j$  label all axonal processes of all LGN cells, and  $\sigma_i \in \{-1, +1\}$  denotes the state of activation of the LGN cell from which process  $i$  emerges, with  $\sigma_i = +1$  ( $-1$ ) denoting activity (inactivity). The patterns of LGN activity are circles of radius  $\rho$  centred on a randomly selected LGN cell with no other LGN cells active. The activated LGN sheet, either left or right, is also selected randomly.

We assume that an energy function exists which characterizes the underlying stochastic dynamics. We take it to be given by

$$E = -\frac{1}{2} \sum_{i,j \neq i} \sigma_i \Delta_{ij} \sigma_j, \quad (1)$$

where  $\Delta_{ij}$  is a function characterizing the diffusion of neurotrophic factors through the target field and is given by

$$\Delta_{ij} = \begin{cases} \exp(-r_{ij}^2/2\sigma_D^2), & \text{for } r_{ij} \leq r_D, \\ 0, & \text{otherwise,} \end{cases} \quad (2)$$

and  $r_{ij}$  is the distance between the processes  $i$  and  $j$  on the array of dendrites, so that if process  $i$  is attached to the dendrite at position  $(X_i, Y_i)$  in the  $cd \times cd$  array of dendrites, and similarly for process  $j$ , then  $r_{ij}^2 = (X_i - X_j)^2 + (Y_i - Y_j)^2$ . The energy  $E_i$  of any particular process  $i$  is implicitly defined. Simultaneously active or inactive processes attached to dendrites separated by a distance  $r_D$  or less decrease  $E$  (we do not require that simultaneous inactivity contributes to  $E$ , but we retain it for reasons of generality), while processes of opposite states of activation increase  $E$ . The parameters  $\sigma_D$  and  $r_D$  will be discussed later. By setting  $\sigma_D = \infty$  and  $r_D = 1$ , we recover the energy function used in our previous work.

The energy function is selected as a simple model of neurotrophic interactions. We suppose that afferent activity promotes the production (Zafra *et al.* 1991; Gwag & Springer 1993) and release (Blöchl & Thoenen 1995; Griesbeck *et al.* 1995) of neurotrophic factors from target cells. The level of correlated afferent activity is taken to determine the amounts of neurotrophic factors released. These factors are then assumed to diffuse rapidly through the target field (cf. Montague *et al.* 1991). This diffusion is characterized by the function  $\Delta_{ij}$  in  $E$ . The parameters  $\sigma_D$  and  $r_D$  characterize the diffusion as a Gaussian hump centred on the release site, with a cut-off beyond a certain point. The energy of an individual process is thus taken as a measure of the levels of neurotrophic factors available, after diffusion, at the target cell on which the process synapses; high energy corresponds to low levels, and low energy corresponds to high levels.

Since the local availability of neurotrophic factors appears to determine, in part, the complexity of afferents' axonal arbors (see, for example, Campenot 1982*a, b*; Cohen-Cory & Fraser 1995), we assume that the energy function determines whether afferents sprout or retract. We assume that the uptake of neurotrophic factors by afferents is rapid. Active processes are assumed to require greater neurotrophic support than inactive ones (cf. Meyer-Franke *et al.* 1995). We will therefore select only active LGN cells as candidates for sprouting and retraction. To model sprouting and retraction, we assume that the dynamics of sprouting and retraction are such that the energy function is minimized. This corresponds to active afferents sprouting into regions of high neurotrophic support (low energy) and retracting from regions of low neurotrophic support (high energy). Energy minimization (neurotrophic support maximization) implements competitive neural dynamics directly, since pairs of axonal processes of opposite states of activation increase the energy (decrease neurotrophic support). We have therefore dispensed with the need for synaptic normalization.

To minimize the energy in a systematic fashion, and so simulate changes in axonal morphology, we employ the machinery of statistical mechanics. Thus, the system is taken to be immersed in a heat bath of temperature  $T$  with the distribution of states of connectivity following the Gibbs distribution (Huang

1987). If sprouting a new process or retracting an old one were to cause an energy change  $\Delta E$ , then the new pattern of connectivity induced by sprouting or retraction is accepted with probability

$$\frac{1}{1 + \exp[(\Delta E - \theta \Delta N)/T]}, \quad (3)$$

where  $\Delta N = +1$  ( $-1$ ) for sprouting (retraction), and  $\theta$  is the chemical potential. The chemical potential may be used to model pharmacological manipulations (Elliott *et al.* 1996*c*), but here we set it to zero. We also set the temperature  $T$  to zero, so that changes in connectivity which lower the energy are always accepted, those which raise the energy are never accepted, and those which leave the energy unchanged are accepted with probability 0.5. In previous work we considered simulated annealing, in which the temperature is initially very high, and slowly reduced to zero (Elliott *et al.* 1996*a*). The temperature may be regarded as a measure of the non-correlation-based plasticity affecting the correlation-based dynamics of the network (an interpretation which we owe to K. D. Miller).

Changes in dendritic morphology are assumed to occur in response to changes in axonal morphology. While we do not consider the possibility of dendritic branching, we do permit changes in the lengths of dendrites in the  $d \times d$  arrays of existing primary dendrites supported by each cortical cell. We assume that the length of a dendrite is proportional to the number of synapses it supports. The justification for this is as follows. In order for a synapse to remain in existence, the pre-synaptic terminal requires adequate neurotrophic support (low energy), otherwise it will be retracted. In order for a new process to be formed and maintained, the dendrite (or cell) must elevate the overall level of neurotrophic support. However, preliminary evidence suggests that neurotrophic factors may be involved in regulating dendritic as well as axonal growth (Snider 1988; McAllister *et al.* 1995, 1996). Thus, if we assume that the target cell's neurotrophic factor production and release is involved in regulating its own dendritic growth, then dendrites will be more numerous and complex in regions of higher innervation density than in regions of lower innervation density. That is, we need only assume that increased levels of neurotrophic factors act not only to sustain more axonal processes but also to promote the growth of the dendrites on which new processes form synapses. For simplicity, we consider that this growth is reflected only in a change in the lengths of dendrites.

We stress that our taking dendritic length to be proportional to the number of synapses is an interpretation. For the purposes of our computational procedures, dendrites are, in fact, regarded as zero-dimensional objects. However, assigning a length to a dendrite would seem to raise the possibility of permitting different levels of neurotrophic factor release along the length of the dendrite. Furthermore, we must interpret the dendritic growth as being perpendicular to the underlying two-dimensional array of cortical cells, so that we can continue to regard



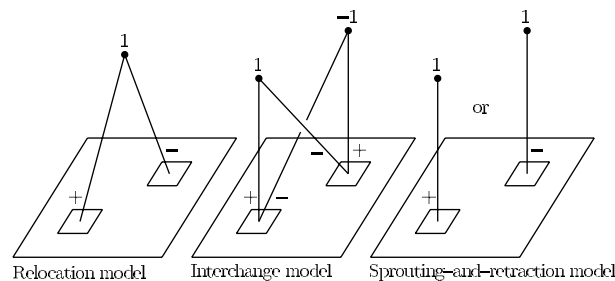


Figure 1. A graphical summary of the strategies for sprouting and retraction in the three models discussed in the text. The sheets denote the cortex, while the blobs denote LGN cells. Each number represents the state of activation of the associated LGN cell (+1 means that the cell is active, -1 that it is inactive), and a '+' ('-') sign indicates sprouting (retraction).

dendrites as separated by fixed distances. Growth in a third dimension will affect, to some degree, our assumptions regarding diffusion. We have made no attempt to take these possibilities into account. To do so would considerably complicate our analysis.

Our computational procedure, then, is as follows. First an initial pattern of connectivity between the LGN sheets and the cortex is constructed. At this point, each cortical cell is exactly binocularly driven. Correspondingly, all dendritic lengths are interpreted to be equal. Then an LGN sheet is randomly activated as described above. This is followed by considering five random sproutings and five random retractions from active LGN cells; within the restriction that the number of sproutings and retractions per LGN activation should not be too large, these numbers are chosen for reasons of computational convenience. Whether each change in connectivity is performed is determined by comparing the probability generated by equation (3) with a random number in the interval between zero and one, inclusive. A change in axonal morphology is interpreted as inducing a change in the lengths of relevant dendrites. This whole process of random LGN activation followed by stochastic updating is repeated  $2.5 \times 10^6$  times.

Since sprouting and retraction can occur independently, we call the model presented here the 'sprouting-and-retraction' model. Previously, in models based on the same framework, sprouting and retraction were always coupled, leading to a conservation of the number of axonal processes supported by each axon. We called these models the 'relocation' model and the 'interchange' model. These different models are graphically summarized in figure 1. The advantage of the present sprouting-and-retraction model is that anomalous peripheral activity, such as that induced by monocular deprivation, can be simulated without hand-setting any parameters (Elliott *et al.* 1996c).

In order to calculate a bias index which quantifies the asymmetry of a cell's dendritic field, we follow closely the method used experimentally (Katz *et al.* 1989; Kossel *et al.* 1995). One takes a picture of a stained cortical cell and draws a series of concentric

circles of uniformly increasing radius, centred on the cell soma. Then one partitions the dendritic field into two regions by drawing a line through the soma parallel to the nearest ocular dominance column boundary. The number of intersections between each hemisphere and the dendrites is counted, and a total obtained for all dendrites pointing towards the boundary,  $N_{\text{to}}$ , and for all dendrites pointing away from the boundary,  $N_{\text{away}}$ . Katz *et al.* (1989) then define the bias index to be  $b_{\text{Katz}} = N_{\text{away}}/N_{\text{to}}$ , while Kossel *et al.* (1995) define it to be  $b_{\text{Kossel}} = N_{\text{away}} - N_{\text{to}}$ . We prefer to define it as  $b = (N_{\text{away}} - N_{\text{to}})/(N_{\text{away}} + N_{\text{to}})$ , which is the relative difference and thus has the advantage of taking values in the interval  $[-1, +1]$  and being independent of the absolute number of dendritic intersections.  $b_{\text{Katz}}$  may be obtained from  $b$  by using the relation  $b_{\text{Katz}} = (1 + b)/(1 - b)$ . If  $b = +1$  ( $-1$ ), then there is complete bias away from (towards) a boundary, and  $b = 0$  means a perfectly symmetric dendritic field.

Computationally, because the simulated dendrites are visualized differently from real dendrites, we count the number of synapses supported by a dendrite, which we take to be proportional to its length. If a dendrite lies on the line dividing the dendritic field in two, then half the synapses are counted as 'away', and half are counted as 'towards'. We shall, in fact, take  $d = 3$ , so that each cortical cell supports a  $3 \times 3$  array of nine dendrites. This means that we need consider only eight different partitions, corresponding to the horizontal or vertical mid-lines or the two diagonals, with two possible assignments of 'away' and 'towards' for each. Finally, if a cell is equidistant from multiple boundaries, then a bias index is calculated for each possible selection of the nearest boundary.

### 3. RESULTS

In this section we present results obtained from simulations of the sprouting-and-retraction model. We set  $c = 19$ ,  $r = 9$  and  $a = 5$ . There is no qualitative difference in our results for other selections of these parameters. We set  $d = 3$ , giving a  $3 \times 3$  array of dendrites for each cortical cell. The diffusion parameters are set to  $\sigma_{\text{D}} = 2.5$  and  $r_{\text{D}} = 3$ . The former exerts a mild control over column width, while the latter exerts a mild control over the extent of the asymmetry of dendritic fields near column boundaries. We set  $\rho = 2$ , so that at any given time only about 16% of an LGN sheet is active. We discuss larger values of  $\rho$  later.

In figure 2 we show two typical examples of the final pattern of ocular dominance produced by the sprouting-and-retraction model. At the level of dendrites, we find complete segregation of the geniculocortical afferents—each dendrite is controlled by only one eye. At the level of cortical cells, we find almost complete segregation, with a few binocular cells whose dendrites are partitioned into two distinct groups, one group controlled by one eye, the other group by the other eye. Despite the absence of

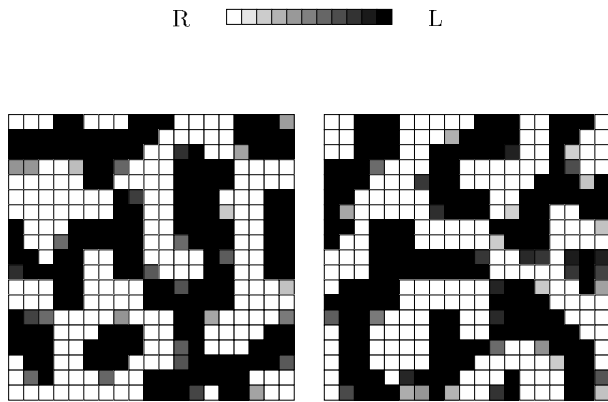


Figure 2. Two examples of the final pattern of ocular dominance produced by the sprouting-and-retraction model. The parameters are:  $c = 19$ ,  $r = 9$ ,  $a = 5$ ,  $d = 3$ ,  $\rho = 2$ ,  $\sigma_D = 2.5$ ,  $r_D = 3$ . Each square in the maps corresponds to one cortical cell, and the darkness indicates the ocularity. White squares are completely controlled by the right eye ('R'), and black squares by the left eye ('L'), with shades of grey interpolating between.

limits on connectivity, except for that requiring that each axon supports a minimum number of processes, we find that the columns are of approximately uniform width and exhibit realistic morphological characteristics, such as branching.

We find that some of the dendrites of cells immediately adjacent to column boundaries are either uninnervated or poorly innervated, while the dendrites of cells away from column boundaries are typically well innervated. Uninnervated dendrites are thought of as having undergone retraction, while well-innervated dendrites are thought of as having undergone activity-dependent growth. This follows from our interpretation that the length of a dendrite is proportional to the number of synapses supported by it.

Figure 3 shows the mean bias index of all monocularly driven cortical cells in both maps in figure 2 as a function of distance from the nearest boundary. A cortical distance of one means that the cell is immediately adjacent to a boundary, a distance of  $\sqrt{2}$  means that the cell is diagonally adjacent to a boundary, and so on. Data for distances greater than two are removed because too few such cells exist in each map for reliable statistics. We see a pronounced bias for small distances and smaller biases consistent with zero for larger distances.

In figure 4 we show six examples of cells with asymmetric dendritic fields and an example of a binocularly controlled cell. For the purposes of visualization we have discarded the central dendrite in the  $3 \times 3$  array and 'flattened' the remaining eight in directions consistent with their relative positions in the array.

In previous work (Elliott *et al.* 1996a) we showed that the relocation model (in which an axon is taken to sprout one process and retract another, giving the impression that the axon has simply relocated the same process; see figure 1) gives rise to envelopes of uninnervated cells surrounding ocular dominance columns. Were we to push the relocation model down

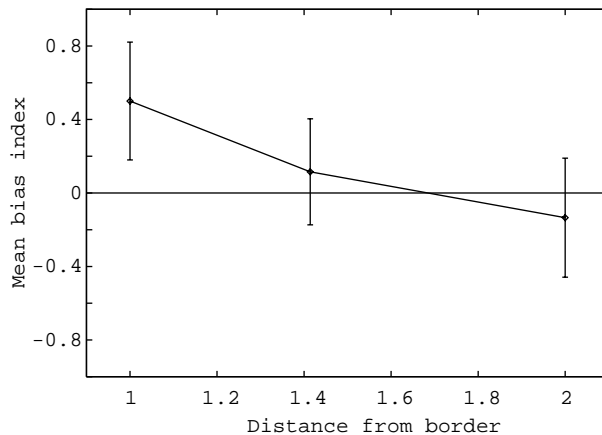


Figure 3. The mean bias index for all monocularly driven cortical cells in both maps of figure 2, plotted as a function of distance from the nearest ocular dominance column boundary. The vertical bars denote standard deviation.

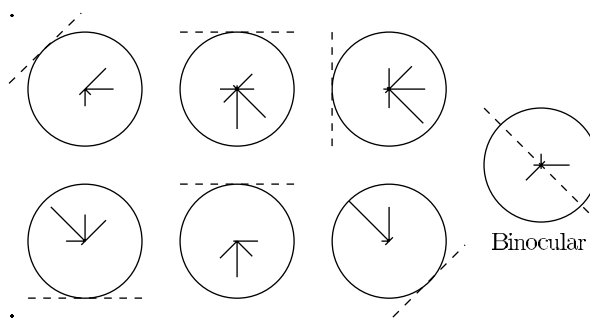


Figure 4. Six examples of biased cortical cell dendritic fields and one example of a binocularly driven cortical cell dendritic field drawn from both maps in figure 2. The circle around each cell represents the length of the longest (that is, most well-innervated) dendrite found on the displayed cells, while the dashed line represents the ocular dominance column boundary.

to the level of dendrites, we would, instead, obtain uninnervated, and thus retracted, dendrites at ocular dominance column boundaries. However, in the relocation model, the bias only becomes significant in the rather extreme stimulation regime when the LGN activation radius  $\rho$  is set to  $\rho = 5$ , for which, alternately, one LGN sheet is completely activated and the other inactivated. As  $\rho$  is reduced, the bias is eliminated. In contrast, the sprouting-and-retraction model discussed here develops a pronounced bias even for small  $\rho$ . Paradoxically, for large  $\rho$ , the bias reduces to near zero (data not shown).

The reasons for this opposed behaviour in both models are subtle. In the relocation model, the relocation rule induces a statistical force of attraction between processes whose activities are correlated, and a statistical force of repulsion between processes of opposite states of activation. Thus, even in the absence of the contribution to  $E$  which raises the energy when processes have opposite activities, and which therefore implements competition in the sprouting-and-retraction model, the non-competitive statistical force of attraction is enough to induce the formation of ocular dominance columns in the relocation model.

For large  $\rho$ , more afferents from the same LGN sheet have correlated activity, with the result that they experience, overall, a greater attraction towards each other and a greater repulsion from afferents from the other LGN sheet. The regions of uninnervated cells (or dendrites) thus constitute gaps across which the repulsive forces cannot be communicated. For small  $\rho$ , the overall statistical forces are too small to induce such gaps. The fact, then, that the relocation model produces increasing dendritic bias for increasing  $\rho$  should not be taken seriously. (See Appendix 1 for an analysis of the statistical forces.)

In the sprouting-and-retraction model discussed here, no such statistical forces exist, because sprouting and retraction are uncoupled. Therefore the dendritic gaps separating different afferents are not merely spaces across which statistical repulsion cannot be communicated. Instead, they represent genuine regions of low neurotrophic support (high energy) induced by ongoing competition between the two eyes. The neurotrophic support in these regions is so low that no processes can be maintained in them. Increasing  $\rho$ , however, increases the overall level of correlated activity within an eye, and elevates neurotrophic support at boundaries to such a level that, while competition continues and deprivation effects are possible, strong innervation at the boundaries becomes feasible. Preliminary indications suggest that permitting inactive as well as active processes to retract, tempers this behaviour. It would be enough to assume that even inactive processes require a resting level of trophic support to justify this further rule.

#### 4. DISCUSSION

In this paper we have extended our previous approach to neural development and plasticity in order to account for the development of the dendritic bias of cortical cells at ocular dominance column boundaries. The central assumption underlying this extension is that changes in dendritic morphology occur in response to changes in axonal morphology. In particular, we have assumed that, where innervation density is low, dendrites are relatively short and unramified, and where innervation density is high, dendrites are relatively long and well ramified.

In order to justify these assumptions, we have proposed a neurotrophic model of the development of both axonal and dendritic arbors. Regions of high innervation density are likely to be associated with significant neurotrophic support (Campenot 1982*a, b*; Cohen-Cory & Fraser 1995). Such levels of neurotrophic support are themselves likely to reflect significant degrees of correlated afferent activity in those regions, since the production and release of neurotrophic factors depends, in part, on afferent activity (Zafra *et al.* 1991; Gwag & Springer 1993; Griesbeck *et al.* 1995; Blöchl & Thoenen 1995). However, recent evidence suggests that dendritic growth might depend, in part, on neurotrophic factors (Snider 1988; McAllister *et al.* 1995, 1996). It

thus seems reasonable to suppose that regions of high innervation density, and therefore high neurotrophic support, are associated with relatively long and well-ramified dendrites. Conversely, regions of poorly correlated afferent activity should be associated with low neurotrophic support and thus low innervation density and relatively short and unramified dendrites. Such a model naturally accounts for the dendritic bias of cortical cells at ocular dominance column boundaries because these are precisely the regions of poorly correlated afferent activity. Furthermore, decreasing the correlations by inducing strabismus should enhance the bias; this is consistent with experimental results (Kossel *et al.* 1995).

The sprouting-and-retraction model suggests that cortical cell dendritic bias does not develop in animals which have experienced very strong intra-ocular image correlations, corresponding to large  $\rho$ . This is because the activities of afferents on either side of the ocular dominance column boundaries are so strongly correlated that neurotrophic factor levels are predicted to be high even at the boundaries, despite the very strong inter-ocular image anti-correlations. This is a very specific prediction of our model, although it is likely to be difficult to test. However, direct stimulation of the optic nerves is possible (Stryker & Strickland 1984) and has recently been shown to interfere with the development of orientation selectivity in the visual cortex (Weliky & Katz 1997). We therefore predict that animals reared with complete but asynchronous stimulation of the optic nerves do not develop a cortical cell dendritic bias. The relocation model predicts the reverse: that the dendritic bias should be enhanced in such a scenario. However, this is, as explained above, likely to be an artifact, and should not be taken seriously.

The idea that changes in dendritic morphology occur in response to changes in axonal morphology makes the specific prediction that the segregation of geniculocortical afferents should occur before or simultaneously with, but not after, the emergence of dendritic bias. It would be of considerable interest to determine the time course of the development of dendritic bias, since it is conceivable that it could provide a partial account for the critical period for a response to monocular deprivation (Hubel & Wiesel 1970). If the distance over which undeprived-eye geniculocortical afferents can sprout in response to monocular deprivation (Friedlander *et al.* 1991; Antonini & Stryker 1996) is limited, then a poorly developed dendritic bias might permit the gradual advance of undeprived-eye afferents into deprived-eye territory, whereas a significant bias might prevent any advance. Thus, if dendritic bias emerges after the segregation of geniculocortical afferents, and if a significant bias prevents the advance of undeprived-eye afferents in response to monocular deprivation, then the emergence of dendritic bias would be causally responsible for the critical period. This possibility thus predicts that animals reared with complete but asynchronous stimulation of the optic nerves, which we suggest might not exhibit a dendritic bias at ocular dominance column boundaries, will continue to



respond to monocular deprivation well beyond the end of the critical period in normally reared animals. Conversely, when dendritic bias is enhanced by strabismus (Kossel *et al.* 1995), we require that the response to monocular deprivation is correspondingly tempered. Evidence does indeed suggest that prior strabismus protects against the effects of monocular deprivation (Mustari & Cynader 1981).

Larger  $\rho$  in the sprouting-and-retraction model is also associated with elevated levels of axonal growth. This is not simply because dendritic bias does not develop: there is greater growth even well away from ocular dominance column boundaries. This phenomenon occurs because the correlated activity within an eye increases. We therefore predict that experimental manipulations of intra-ocular image correlations could also change the innervation density found at the level of the striate cortex. This prediction raises the possibility that varying inter-ocular image correlations might also affect innervation density. We therefore suggest, as an experimentally easier manipulation, that the average number of synapses supported by cortical cells in strabismic cats, particularly at the centres of ocular dominance columns, may be different from that in normally reared cats. That strabismus changes columnar characteristics, in addition to bias (Kossel *et al.* 1995), has already been established (Löwel 1994), with changes in columnar periodicity having been predicted by a model of ocular dominance column formation (Goodhill 1993; Goodhill & Löwel 1995). Our suggestion therefore appears to be a good candidate for experimental testing.

The trigeminal field of the somatosensory cortex in rodents consists of dense regions of neuropil, each region being innervated by one whisker, surrounded by regions of sparse neuropil (Woolsey & Van der Loos 1970; Welker 1976). The dendritic morphology of barrel cortex cells undergoes change in response to peripheral perturbations (Harris & Woolsey 1979; Steffen & Van der Loos 1980). In previous work, we simulated the plasticity exhibited by the mature barrel field (Elliott *et al.* 1996*b*). The approach presented here could also be applied to the barrel cortex, resulting in poorly innervated (and thus retracted) dendrites at barrel boundaries. However, since the post-natal development of the barrel field does not appear to depend on neural activity (Chiaia *et al.* 1992; Henderson *et al.* 1992; Schlaggar *et al.* 1993), we have not presented results for the sprouting-and-retraction model applied to the barrel cortex.

In conclusion, we have shown that a sprouting-and-retraction model based on competition for neurotrophic factors can naturally account for the dendritic bias observed in the ocular dominance column system. We have argued that dendritic bias emerges as competing sets of inputs are spatially separated. We have predicted that dendritic bias emerges after or simultaneously with, but not before, afferent segregation. We predict that animals reared with complete but asynchronous stimulation of the optic nerves do not exhibit dendritic bias. We suggest that the emergence of dendritic bias might pro-

vide a partial account of the critical period. Therefore we require that animals which have been reared with artificially elevated intra-ocular image correlations should respond to monocular deprivation for longer than normally reared animals. We have also suggested that ocular dominance columns in strabismic cats may be differently innervated from those in normally reared cats. This is a prediction which only a sprouting-and-retraction model can make, since fixed-anatomy models do not permit the growth of new connections.

We thank two anonymous referees for many valuable suggestions for improvement of this paper. T.E. thanks the Royal Society for the support of a Royal Society University Research Fellowship during the latter stages of this work.

## APPENDIX 1. STATISTICAL FORCES

The energy  $E_{ij}$  of interaction between two axonal processes  $i$  and  $j$ , in the limit  $r_D \rightarrow \infty$ , is given by

$$E_{ij} = -\sigma_i \sigma_j \exp(-r_{ij}^2/2\sigma_D^2), \quad (4)$$

and the force acting on process  $i$  as a result of the presence of process  $j$  is given by  $\mathbf{F}_{ij} = -\nabla_i E_{ij}$ , where  $\nabla_i = (\partial/\partial X_i, \partial/\partial Y_i)$ , which gives

$$\mathbf{F}_{ij} = -\frac{\sigma_i \sigma_j}{\sigma_D^2} \exp(-r_{ij}^2/2\sigma_D^2) \mathbf{r}_{ij}, \quad (5)$$

where  $\mathbf{r}_{ij} = (X_i - X_j, Y_i - Y_j)$ . This is a central potential, with the force acting along the radius vector. For  $\sigma_i \sigma_j > 0$  (correlated activity), the force is attractive, while for  $\sigma_i \sigma_j < 0$  (anti-correlated activity), the force is repulsive. Averaging over LGN activity, we have that  $\langle \mathbf{F}_{ij} \rangle \propto -C_{ij} \mathbf{r}_{ij}$ , where  $C_{ij} = \langle \sigma_i \sigma_j \rangle$ , and  $\langle \rangle$  denotes averaging. For processes from the same LGN sheet,  $C_{ij}$  increases as  $\rho$  increases (thus, an overall greater attraction), while for processes from opposite LGN sheets,  $C_{ij}$  becomes increasingly negative as  $\rho$  increases (thus, an overall greater repulsion). In our previous work on the relocation model (Elliott *et al.* 1996*a*), we took  $r_D = 1$  and  $\sigma_D = \infty$ . This gives rise to a singular force,  $\mathbf{F}_{ij} = -\sigma_i \sigma_j \delta(r_{ij} - 1) \mathbf{r}_{ij}$ , but the arguments are essentially unchanged.

We call these forces ‘statistical’ because the relocation rule (see figure 1)—an axon sprouting in one place and retracting from another—arises purely statistically. That is, relocation is only apparent, not real. We are not, therefore, suggesting that real forces of attraction and repulsion may exist between real axon terminals (except due to their electrical properties), but that, if anything like the relocation of processes is a good way of thinking about neural plasticity, then such forces will appear to exist.

In principle, a similar analysis goes through for the sprouting-and-retraction model. However, the sprouting and retraction rules do not permit axon terminals to move, but just to appear and disappear. Thus, the notion of statistical forces affecting motion cannot be formulated. The relocation rule permits the identification of a stable object whose motion across the cortex may be followed. This then permits the notion of statistical forces to emerge.



## REFERENCES

- Antonini, A. & Stryker, M. P. 1996 Plasticity of geniculocortical afferents following brief or prolonged monocular occlusion in the cat. *J. Comp. Neurol.* **369**, 64–82.
- Bear, M. F. & Colman, H. 1990 Binocular competition in the control of geniculate cell size depends upon visual cortical N-methyl-D-aspartate receptor activation. *Proc. Natn. Acad. Sci. USA* **87**, 9246–9249.
- Bear, M. F., Kleinschmidt, A., Gu, Q. & Singer, W. 1990 Disruption of experience-dependent synaptic modifications in striate cortex by infusion of an NMDA receptor antagonist. *J. Neurosci.* **10**, 909–925.
- Bienenstock, E. L., Cooper, L. N. & Munro, P. W. 1982 Theory for the development of neuron selectivity: orientation specificity and binocular interaction in visual cortex. *J. Neurosci.* **2**, 32–48.
- Blöchl, A. & Thoenen, H. 1995 Characterization of nerve growth factor (NGF) release from hippocampal neurons: evidence for a constitutive and an unconventional sodium-dependent regulated pathway. *Eur. J. Neurosci.* **7**, 1220–1228.
- Bozzi, Y., Pizzorusso, T., Cremisi, F., Rossi, F. M., Barsacchi, G. & Maffei, L. 1995 Monocular deprivation decreases the expression of messenger RNA for brain-derived neurotrophic factor in the rat visual cortex. *Neuroscience* **69**, 1133–1144.
- Cabelli, R. J., Hohn, A. & Shatz, C. J. 1995 Inhibition of ocular dominance column formation by infusion of NT-4/5 or BDNF. *Science* **267**, 1662–1666.
- Campenot, R. B. 1982a Development of sympathetic neurons in compartmentalized cultures. I. Local control of neurite outgrowth by nerve growth factor. *Dev. Biol.* **93**, 1–12.
- Campenot, R. B. 1982b Development of sympathetic neurons in compartmentalized cultures. II. Local control of neurite survival by nerve growth factor. *Dev. Biol.* **93**, 13–22.
- Carmignoto, G., Canella, R., Candeo, P., Comelli, M. C. & Maffei, L. 1993 Effects of nerve growth factor on neuronal plasticity of the kitten visual cortex. *J. Physiol.* **464**, 343–360.
- Castren, E., Zafra, F., Thoenen, H. & Lindholm, D. 1992 Light regulates expression of brain-derived neurotrophic factor mRNA in rat visual cortex. *Proc. Natn. Acad. Sci. USA* **89**, 9444–9448.
- Changeux, J. P. & Danchin, A. 1976 Selective stabilization of developing synapses as a mechanism for the specification of neural networks. *Nature* **264**, 705–712.
- Chiaia, N. L., Fish, S. E., Bauer, W. R., Bennett-Clarke, C. A. & Rhoades, R. W. 1992 Postnatal blockade of cortical activity by tetrodotoxin does not disrupt the formation of vibrissa-related patterns in the rat's somatosensory cortex. *Dev. Brain Res.* **66**, 244–250.
- Clothiaux, E. E., Bear, M. F. & Cooper, L. N. 1991 Synaptic plasticity in visual cortex: comparing theory with experiment. *J. Neurophysiol.* **66**, 1785–1804.
- Cohen-Cory, S. & Fraser, S. E. 1995 Effects of brain-derived neurotrophic factor on optic axon branching and remodelling *in vivo*. *Nature* **378**, 192–196.
- Elliott, T., Howarth, C. I. & Shadbolt, N. R. 1996a Axonal processes and neural plasticity. I. Ocular dominance columns. *Cerebr. Cortex* **6**, 781–788.
- Elliott, T., Howarth, C. I. & Shadbolt, N. R. 1996b Axonal processes and neural plasticity. II. Adult somatosensory maps. *Cerebr. Cortex* **6**, 789–793.
- Elliott, T., Howarth, C. I. & Shadbolt, N. R. 1996c Neural competition and statistical mechanics. *Proc. R. Soc. Lond. B* **263**, 601–606.
- Fraser, S. E. & Perkel, D. H. 1989 Competitive and positional cues in the patterning of nerve connections. *J. Neurobiol.* **21**, 51–72.
- Friedlander, M. J., Martin, K. A. C. & Wassenhove-McCarthy, D. 1991 Effects of monocular visual deprivation on geniculocortical innervation of area 18 in cat. *J. Neurosci.* **11**, 3268–3288.
- Goodhill, G. J. 1993 Topography and ocular dominance: a model exploring positive correlations. *Biol. Cybern.* **69**, 109–118.
- Goodhill, G. J. & Löwel, S. 1995 Theory meets experiment: correlated neural activity helps determine ocular dominance column periodicity. *Trends Neurosci.* **18**, 437–439.
- Griesbeck, O., Blöchl, A., Carnahan, J. F., Nawa, H. & Thoenen, H. 1995 Characterization of brain-derived neurotrophic factor (BDNF) secretion from hippocampal neurons. *Soc. Neurosci. Abs.* **21**, 1046.
- Gwag, B. J. & Springer, J. E. 1993 Activation of NMDA receptors increases brain-derived neurotrophic factor (BDNF) mRNA expression in the hippocampal formation. *NeuroReport* **5**, 125–128.
- Harris, R. M. & Woolsey, T. A. 1979 Morphology of Golgi-impregnated neurons in mouse cortical barrels following vibrissae damage at different post-natal ages. *Brain Res.* **161**, 143–149.
- Hata, Y. & Stryker, M. P. 1994 Control of thalamocortical afferent rearrangement by postsynaptic activity in developing visual cortex. *Science* **265**, 1732–1735.
- Henderson, T. A., Woolsey, T. A. & Jacquin, M. F. 1992 Infraorbital nerve blockade from birth does not disrupt central trigeminal pattern formation in the rat. *Dev. Brain Res.* **66**, 146–152.
- Hopfield, J. J. 1982 Neural networks and physical systems with emergent collective computational abilities. *Proc. Natn. Acad. Sci. USA* **79**, 2554–2558.
- Huang, K. 1987 *Statistical mechanics*. London: Wiley.
- Hubel, D. H. & Wiesel, T. N. 1962 Receptive fields, binocular interaction and functional architecture in the cat's visual cortex. *J. Physiol.* **160**, 106–154.
- Hubel, D. H. & Wiesel, T. N. 1970 The period of susceptibility to the physiological effects of unilateral eye closure in kittens. *J. Physiol.* **260**, 419–436.
- Katz, L. C. & Constantine-Paton, M. 1988 Relationships between segregated afferents and postsynaptic neurons in the optic tectum of three-eyed frogs. *J. Neurosci.* **8**, 3160–3180.
- Katz, L. C., Gilbert, C. D. & Wiesel, T. N. 1989 Local circuits and ocular dominance columns in monkey striate cortex. *J. Neurosci.* **9**, 1389–1399.
- Kleinschmidt, A., Bear, M. F. & Singer, W. 1987 Blockade of 'NMDA' receptors disrupts experience-dependent plasticity of kitten striate cortex. *Nature* **238**, 355–358.
- Kossel, A., Löwel, S. & Bolz, J. 1995 Relationships between dendritic fields and functional architecture in striate cortex of normal and visually deprived cats. *J. Neurosci.* **15**, 3913–3926.
- LeVay, S., Stryker, M. P. & Shatz, C. J. 1978 Ocular dominance columns and their development in layer IV of the cat's visual cortex: a quantitative study. *J. Comp. Neurol.* **179**, 223–244.
- LeVay, S., Wiesel, T. N. & Hubel, D. H. 1980 The development of ocular dominance columns in normal and visually deprived monkeys. *J. Comp. Neurol.* **191**, 1–51.
- Löwel, S. 1994 Ocular dominance column development: strabismus changes the spacing of adjacent columns in cat visual cortex. *J. Neurosci.* **14**, 7451–7468.

- McAllister, A. K., Lo, D. C. & Katz, L. C. 1995 Neurotrophins regulate dendritic growth in developing visual cortex. *Neuron* **15**, 791–803.
- McAllister, A. K., Katz, L. C. & Lo, D. C. 1996 Neurotrophin regulation of cortical dendritic growth requires activity. *Neuron* **17**, 1057–1064.
- Meyer-Franke, A., Kaplan, M. R., Pfrieger, F. W. & Barnes, B. A. 1995 Characterization of the signaling interactions that promote the survival and growth of developing retinal ganglion cells in culture. *Neuron* **15**, 805–819.
- Montague, P. R., Gally, J. A. & Edelman, G. M. 1991 Spatial signaling in the development and function of neural connections. *Cerebr. Cortex* **1**, 199–220.
- Mustari, M. & Cynader, M. 1981 Prior strabismus protects kitten cortical neurons from the effects of monocular deprivation. *Brain Res.* **211**, 165–170.
- Purves, D. 1988 *Body and brain: a trophic theory of neural connections*. Cambridge, MA: Harvard University Press.
- Purves, D. 1994 *Neural activity and the growth of the brain*. Cambridge University Press.
- Riddle, D. R., Lo, D. C. & Katz, L. C. 1995 NT-4-mediated rescue of lateral geniculate neurons from effects of monocular deprivation. *Nature* **378**, 189–191.
- Schlaggar, B. L., Fox, K. & O'Leary, D. D. M. 1993 Postsynaptic control of plasticity in developing somatosensory cortex. *Nature* **364**, 623–626.
- Schoups, A. A., Elliott, R. C., Friedman, W. J. & Black, I. B. 1995 NGF and BDNF are differentially modulated by visual experience in the developing geniculocortical pathway. *Dev. Brain Res.* **86**, 326–334.
- Snider, W. D. 1988 Nerve growth factor enhances dendritic arborization of sympathetic ganglion cells in developing mammals. *J. Neurosci.* **8**, 2628–2634.
- Steffen, H. & Van der Loos, H. 1980 Early lesions of mouse vibrissal follicles: their influence on dendrite orientation in the developing barrelfield. *Expl Brain Res.* **40**, 410–431.
- Stryker, M. P. & Strickland, S. L. 1984 Physiological segregation of ocular dominance columns depends on the pattern of afferent electrical activity. *Invest. Ophthalmol. Vis. Sci.* (Suppl.) **25**, 278.
- Tanaka, S. 1991 Theory of ocular dominance column formation: mathematical basis and computer simulation. *Biol. Cybern.* **64**, 263–272.
- Von der Malsburg, C. 1973 Self-organization of orientation selective cells in the striate cortex. *Kybernetik* **14**, 85–100.
- Von der Malsburg, C. 1979 Development of ocularity domains and growth behavior of axon terminals. *Biol. Cybern.* **32**, 49–62.
- Weliky, M. & Katz, L. C. 1997 Disruption of orientation tuning in visual cortex by artificially correlated neuronal activity. *Nature* **386**, 680–685.
- Welker, C. 1976 Receptive fields of barrels in the somatosensory neocortex of rat. *J. Comp. Neurol.* **166**, 173–190.
- Woolsey, T. A. & Van der Loos, H. 1970 The structural organization of layer IV in the somatosensory region (SI) of mouse cerebral cortex. The description of a cortical field composed of discrete cytoarchitectonic units. *Brain Res.* **17**, 205–242.
- Zafra, F., Castren, E., Thoenen, H. & Lindholm, D. 1991 Interplay between glutamate and  $\gamma$ -aminobutyric acid transmitter systems in the physiological regulation of brain-derived neurotrophic factor and nerve growth factor synthesis in hippocampal neurons. *Proc. Natn. Acad. Sci. USA* **88**, 10 037–10 041.

Received 4 November 1996; accepted 2 May 1997

BIOLOGICAL  
SCIENCES



THE ROYAL  
SOCIETY

PHILOSOPHICAL  
TRANSACTIONS  
OF

BIOLOGICAL  
SCIENCES



THE ROYAL  
SOCIETY

PHILOSOPHICAL  
TRANSACTIONS  
OF